UDC 621.3.013 https://doi.org/10.20998/2074-272X.2025.3.07

X.C. Nguyen, D.T. Le

# Adaptive finite-time synergetic control for flexible-joint robot manipulator with disturbance inputs

***Introduction.*** *In this paper, the adaptive finite time controller is designed for flexible-joint manipulator (FJM) to stabilize oscillations and track the desired trajectory based on synergetic control theory (SCT) under disturbance inputs. The problem of the proposed work consists in the development of a mathematical model of the flexible joint while ignoring the nonlinear components of the actuator and synthesizing the control law that ensures the system stability within a settling time. The* ***aim*** *of this study is to use finite-time synergetic controller to ensure the reduction of system tracking error, avoid vibration and achieve steady state in a certain time period. An adaptive synergetic law is developed to solve the problem of uncertainty in the mathematical model of the actuator of FJM and input disturbances.* ***Methodology.*** *First, based on SCT the finite-time controller is constructed via the functional equation of the first manifold. The control law is designed to ensure the movement of the closed-loop system from an arbitrary initial state into the vicinity of the desired attractive invariant manifold, that is, the target attracting manifold. Secondly, to adjust the control law online, an adaptive law is developed to estimate the disturbance acting on the input. Then, the Lyapunov function is used to prove that the system can be stabilized in a sufficiently small neighborhood of the origin within finite time under input disturbances.* ***Novelty****. The implemented controller is effective in ensuring stability over a given time, minimizing the jitter problem while maintaining tracking accuracy and system robustness in the presence of input noise.* ***Results.*** *Numerical simulation and experimental results are presented to illustrate the effectiveness of the proposed method. The research directions of the model were determined for the subsequent implementation of the results in experimental samples.* References 25, table 1, figures 7.

*Key words:* **flexible-joint manipulator, synergetic control theory, finite-time control, Lyapunov function, adaptive control.**

***Вступ****. У роботі розроблено адаптивний кінцевий регулятор часу для гнучкого шарнірного маніпулятора (FJM) для стабілізації коливань та відстеження бажаної траєкторії на основі синергетичної теорії управління (SCT) при вхідних збуреннях. Завдання пропонованої роботи полягає у розробці математичної моделі гнучкого шарніра з ігноруванням нелінійних складових приводу та синтез закону управління, що забезпечує стійкість системи протягом часу встановлення.* ***Метою*** *даного дослідження є використання кінцевочасного синергетичного регулятора для забезпечення зниження помилки відстеження системи, виключення вібрації та досягнення стійкого стану за певний проміжок часу. Розроблено адаптивний синергетичний закон для вирішення проблеми невизначеності в математичній моделі приводу FJM та вхідних збурень.* ***Методологія****. По-перше, на основі SCT будується кінцевий регулятор часу за допомогою функціонального рівняння першого різноманіття. Закон управління розроблений для забезпечення переміщення замкнутої системи з довільного початкового стану в область бажаного притягуючого інваріантного різноманіття, тобто цільового різноманіття. По-друге, для налаштування закону управління в режимі онлайн розробляється адаптивний закон для оцінки обурення, що діє на вході. Потім за допомогою функції Ляпунова доводиться, що система може бути стабілізована у досить малої околиці початку координат за кінцевий час при вхідних збуреннях.* ***Новизна****. Реалізований регулятор ефективний для забезпечення стійкості протягом заданого часу, мінімізуючи проблему коливань, зберігаючи точність відстеження та надійність системи за наявності вхідного шуму.* ***Результати****. Наведено чисельне моделювання та експериментальні результати для ілюстрації ефективності запропонованого методу. Визначено напрями досліджень моделі для подальшої реалізації результатів у експериментальних зразках.* Бібл. 25, табл. 1, рис. 7.

*Ключові слова:* **гнучко-шарнірний маніпулятор, синергетична теорія управління, кінцевий час управління, функція Ляпунова, адаптивне управління.**

**1. Introduction.** Nowadays, robotic technology has developed strongly, flexible-joint manipulator (FJM) have been widely used in mechatronic systems. Compared to traditional robot joint drive systems, FJM has smaller structures and lighter weights. FJMs are typical representatives of nonlinear coupling systems, which have complex dynamic relationships between rigid links and flexible joints. In these systems, the joints are often driven by elastic mechanisms such as speed reducers or cables [1], and joints with torsional stiffness are known as flexible joints. The existence of joint flexibility causes oscillations in the output of the system. Reducing output oscillation and improving control quality of flexible joints has become a topical issue of interest to many researchers [2].

To achieve high quality control of servo systems, most control methods require establishing an accurate dynamic model. The modeling and control of single disturbances in flexible joint robot controllers have been extensively studied in many researches [3–11]. In [3] the influence of friction force on the control moment of the FJM system is considered. In [4] the dynamic modeling and analytical modeling for robot manipulators with rigid links and flexible joints are presented. Dynamic equations of flexible-joints are firstly developed using the Lagrangian formulation in minimal joint and motor coordinates. In [6] presents a way to derive a low-order model for multi-space serial arms. Due to the low number of degrees of freedom, this model can be used in real-time systems for control and estimation. To build a more accurate dynamic model, work [7] considers the flexibility of the load. Many researches indicate that small power motors are always prioritized as joint actuators to make the mechanical structure compact enough in the design of robot controllers. Consequently, this leads to the fact that joint actuators cannot provide arbitrarily large torque as required by the unconstrained control laws proposed in most previous controllers. In [8, 9] the presence of actuator dynamics is not considered in controller calculations, assuming motor torque is proportional to the voltage supplied to the actuator, simplifying the mathematical model in the synthesis of control laws. In many real-world situations, flexible joint controllers do not account for motor dynamics and input disturbances. If these impacts on torque are ignored in the control method design, the performance of the FJM controller system will decrease, which can lead to a reduction in the system's control quality. Therefore,

practical problems require considering motor dynamic uncertainties and input disturbances when designing controllers for FJM.

In recent years, many researches have presented control laws have been designed to improve the control quality performance of FJM systems, such as PID controller [10], fuzzy logic controller (FLC) [11–13], sliding mode control [8, 14, 15], backstepping control [9, 16, 17], robust control [18], intelligent control [19], synergetic controller [20, 21] and adaptive control [22]. For example, in [10] the authors designed a PID controller, similar to a rigid robot for the flexible joint robot system, and its effectiveness was demonstrated through simulation. In [12], the authors proposed an adaptive FLC using the backstepping approach and dynamic surface method. In [8], an adaptive SMC was proposed, which improves tracking quality under disturbances and is implemented on a real system. In [15], a finite-time sliding mode controller is designed in combination with a disturbance observer to enhance control quality. A novel hybrid control strategy for single-link flexible articulated robot manipulators, addressing the inherent uncertainties and nonlinear dynamics. By integrating nonlinear reduced-order active disturbance rejection control with backstepping control is presented in the paper [16]. In [18], a robust model predictive controller scheme for flexible joint robots modeled as nonlinear Lipschitz systems with unknown bounded perturbations is designed. In [19], a neural network control method was presented for the flexible joint controller system under disturbance conditions. In research [20], synergetic control theory (SCT) was applied with the proposed sliding manifolds. This research show the control system has high robustness, but they do not consider stabilization time and input disturbances. The research on flexible joint controllers that account for input disturbances and stabilization time are still limited. In [22], a generalized adaptive saturated controller based on backstepping control, singular perturbation separation, and neural networks was designed to achieve tracking control with limited torque inputs.

**Purpose and objectives of the article**. With the requirement of ensuring the stability of the FJM system in a given time and overcoming the effects of input disturbances and actuator uncertainties. This work proposes a adaptive finite-time synergetic controller to overcome the effects of external disturbances and ensure the stability time, the adaptive control law compensates the disturbance observed at the system input. The main contribution of this study is to develop a controller by constructing manifolds that satisfy the functional equations that ensure a predetermined convergence time, while simultaneously resisting disturbances and reducing static errors, with the best performance and chattering reducing. In addition, the adaptive control law has been used in the ensemble controller to identify input disturbances and actuator uncertainties. The main objective of this work is to evaluate the effectiveness of the proposed control law for the FJM system. Second, deploy and validate the control law on a real system. The Lyapunov method is used to prove the stability, with the contributions of the work highlighted by:

1) The manifold design using regression and functional equations ensures the finite-time stable system to improve the control accuracy, finite-time convergence and fast transient response.

2) The stability analysis is proven according to the Lyapunov criterion, in which the adaptive law is generated.

3) The control law is realized on an embedded system to verify the effectiveness of the proposed control law.

**2. Methods**.

**2.1. Concept of finite-time control.**

There is a nonlinear system that can be described as:

$$\boldsymbol{x}(t) = f(\boldsymbol{x}(t), \boldsymbol{u}),\ \boldsymbol{x}(0) = \boldsymbol{x}_0, \tag{1}$$

where $\boldsymbol{x} \in R^n$ is the state variable vector and $f(0, 0) = 0$, $\boldsymbol{u} \in R^p$ is the control signal; $f(\boldsymbol{x}, 0) = 0$ is the continuously nonlinear function in an open neighborhood near the origin. If the convergence time is limited by a function $T(\boldsymbol{x}_0)$, the system without input impact is considered finite-time stable. In other words, the system can achieve convergence with certain predetermined time constants denoted by $T_{\max}$, where $T_{\max}$ is a constant satisfying $T(\boldsymbol{x}_0) < T_{\max}$.

**Lemma 1** [25]. Consider the system (1), when $\boldsymbol{u} = 0$ and suppose there exist a Lyapunov function $V(\boldsymbol{x})$, $c>0$, $k>0$ and $0 < \alpha < 1$ such that

$$\dot{V}(\boldsymbol{x}) + cV^{\alpha}(\boldsymbol{x}) + kV(\boldsymbol{x}) \le 0 \tag{2}$$

holds. Then, the equilibrium is finite-time stable and the convergence time is given by

$$T_x(\boldsymbol{x}_0) \le \frac{\ln\left(1 + (k/c)V^{1-\alpha}(\boldsymbol{x}_0)\right)}{k(1-\alpha)}. \tag{3}$$

Similarly, the origin $U = D = R^n$ and $V(\boldsymbol{x})$ is globally finite-time stable if and only if and is radially unbounded.

**2.2. Synergetic control law design process.** The main steps of the STC controller synthesis process can be summarized as follows [19, 23, 24]. Assume the controlled system is described by the nonlinear differential equation system in the form (3). First, by defining a manifold as a function $\psi_1(\boldsymbol{x})$, the control law is designed to force the system to move to the manifold $\psi_1(\boldsymbol{x}) = 0$. The designer can select the manifold type with characteristics according to the desired control quality criteria. In specific cases, the manifold may be a simple linear combination of the state variables.

When the system has not reached technological maturity, continue the same process, defining $m$ manifolds (with $p \le n–1$) sequentially in a decreasing order. The synthesized controller will ensure the system converges to the next manifold $\psi_2$ and then to $\psi_m$. On the final manifold, the system will ensure movement along $\psi_m$ towards the origin. These manifolds will have dynamic characteristics satisfying the equation of the form:

$$T_i\dot{\psi}_i + F_i(\psi_i) = 0, T_i > 0, \tag{4}$$

where $T_i$ is the parameter that affects the rate of convergence to the manifold specified by the macro variable. Simultaneously, the functions $F_i(\psi_i)$ must satisfy the following conditions: $F_i(0) = 0$ and $F_i(\psi_i)(\psi_i)$ for all $\psi_i = 0$, meaning equation (4) is globally asymptotically stable. Additionally, the functions $F_i(\psi_i)$ are chosen in such a way that they satisfy the requirements of the control problem.

The process of designing the control law for system (1) with $p = 1$ is performed as follows: First, take the derivative of the manifold $\psi_i(\boldsymbol{x}) = 0$ and substitute it into (4) combined with system (1) to obtain:

$$T_1 \frac{\partial \psi_1}{\partial t} f_1(\boldsymbol{x}, u) + F_1(\psi_1) = 0\,. \qquad (5)$$

Solving (5) we find the control law $u$. With such a control law, the system enters the first manifold, leading to system (1) being partitioned into a subsystem of a lower order than the original system. Continue the steps above with the partitioned subsystems until the final manifold is reached to obtain the complete control law of the system.

In this design process, each manifold introduces a new constraint in the state space and reduces the order of the control system, operating towards global stability. The quality of the system can be determined through the form of the functional equation and the form of the manifold. As presented above, the settling time can be predetermined through the choices of functional equation forms. The process summarized here can be easily implemented as a computer program for automatic control law synthesis or can be manually executed for simple systems, such as the synthesis of control for a two-degree-of-freedom FJM.

**2.3. Platform introduction and operating principle.** In this paper, the flexible joint system built in the laboratory is taken as the research object (Fig. 1), and the nominal parameters of the system are approximately determined, with the model of the DC motor not fully identified. The motor is considered as a proportional link between the output torque and the input voltage. The prototype of the FJM system and the experimental setup are shown in Fig. 1. The system includes a FMJ system, an OMRON E6B2-CWZ6C 1000 (*P/R*) rotary encoder sensor, a 385-P16 Hall magnet encoder sensor, a BTS 7960 motor control power amplifier circuit, a 775 planetary gear reducer motor, and power supply circuits of 3.3 V and 12 V.

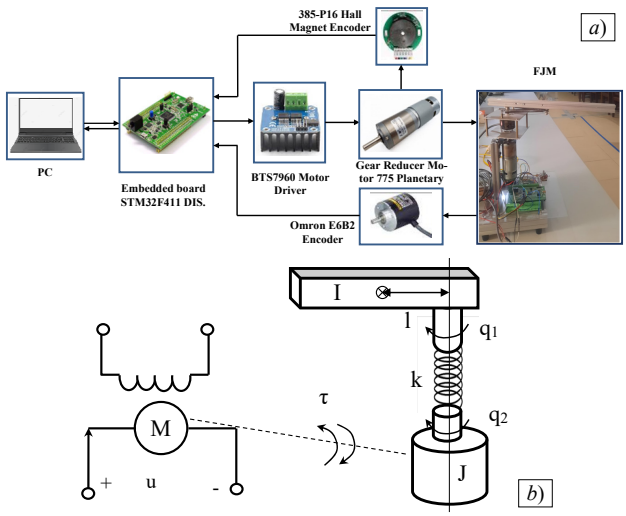


Fig. 1. FJM: *a* – block diagram; *b* – schematic diagram

The STM32F411 embedded board is used as the main board of the real-time control model system. This embedded board has a system frequency of up to 100 MHz and a high-performance 32-bit CPU. The embedded board is the core of the experimental platform and is used to implement real-time algorithms. A large number of peripheral interfaces make the STM32F411 not only capable of good data processing but also facilitate the design of digital systems. The control program is written in C language on the STM32CubeIDE software. Experimental data readings are displayed on MATLAB software through UART communication with a baud rate of 9600 bit/s. The rotational angle data of the link and motor shaft are collected through 2 encoders and read through the interrupt pins of the embedded board. The control algorithm is implemented in embedded software. The control signal is modulated in pulse-width modulation from the general-purpose input/output pins of the embedded board to the voltage amplifier and then to the motor and actuate the link of the FJM.

**2.4. Mathematical model of the FJM.** This section refers to works [8, 14]. The basis of the controller determines the angular position of the flexible link controlled by a direct current motor with an encoder, while the flexible link will respond based on the action of the motor shaft. The deviation of the soft link response is determined by the stiffness of the joint. Due to unknown motor parameters, it is assumed that the output torque is proportional to the voltage applied to the motor, and its joint can only deform when rotating in the vertical plane in the direction of the joint's rotation. Assuming that the frictional force between the links is very small and can be neglected and the states can be measured, the dynamic equation of the FJM takes the form [9, 21]:

$$\begin{cases} I\ddot{q}_1 + mgl\sin(q_1) + k(q_1 - q_2) = 0; \\ J\ddot{q}_1 - k(q_1 - q_2) = \tau + d, \end{cases} \qquad (6)$$

where $q_1$, $q_2$ are the rotation angles of the 2 links of the FJM in Fig. 1. The coefficient $k$ is the stiffness of the flexible joint controller model. The larger the elastic stiffness $k$, the larger the elastic stiffness and the smaller the flexibility of the flexible joint, and $q_1$ is closer to $q_m$. The smaller the $k$, the smaller the elastic stiffness of the flexible joint, the greater the flexibility, and the easier it is to bend the soft arm. $I$ and $J$ are the moments of inertia of the flexible link and the motor rotor; $m$ is the mass of the flexible link; $l$ is the distance from the center of the flexible link to the flexible – joints; $g$ is the gravitational acceleration; $\tau$ is the control torque generated by the motor. In this research, the motor model is not used in the synthesis of the control law, assuming $\tau$ is proportional to the voltage supplied to the motor, meaning $\tau = N{\cdot}u$, in there $u$ is the voltage supplied to the motor and $N$ is the coefficient; $d$ is the control torque disturbance and the uncertainty of the motor model.

We define $x_1 = q_1; x_2 = \dot{q}_1; x_3 = q_2; \dot{x}_4 = \dot{q}_2$. The system of equations of FJM (6) is rewritten as:

$$\begin{cases} \dot{x}_1 = x_2; \\ \dot{x}_2 = -\dfrac{k}{I}x_1 - \dfrac{mgl}{I}\sin x_1 + \dfrac{k}{I}x_3; \\ \dot{x}_3 = x_4; \\ \dot{x}_4 = \dfrac{k}{J}(x_1 - x_3) + \dfrac{N}{J}u + \dfrac{d}{J}. \end{cases} \qquad (7)$$

**Assumption 1.** The unmeasurable factor $d$ is bounded: $|d| = D_{\max}$, where $D_{\max}$ is positive constant.

**Assumption 2.** If $x_1 = 0$; $x_2 = 0$ and $\dot{x}_2 \to 0$ then $x_3 \to 0$.

The model above shows that the system is complex and non-linear. Importantly, the state vector elements are connected to each other through a chained integration procedure and the last state variable can be obtained by integrating the control input $u$. The objective of the FJM control problem is that the angle $q_1$ of link rotates correctly according to the desired signal, the setting time is within the given time $t_f$ and while maintaining control quality under input disturbance $d$.

**2.5. Synthesis of finite-time control law based on SCT without input disturbance.** In this section, the FJM control problem is to ensure that link $q_1$ moves according to the desired trajectory $x_{sp}$ by adjusting the voltage $u$ supplied to the motor to create a torque acting on link $q_2$. Under the effect of the motor torque acting on link $q_2$ to bring the system to the desired point in a finite time and keep the system stable at that position. First, the control law is designed when there is no disturbance, which means $d = 0$. From the perspective of SCT, this means that it is necessary to synthesize the control signal $u(\boldsymbol{x})$. The action of the control law will move the links through the joints from the initial position following a given signal or stabilize at the desired position when there is a disturbance to ensure control quality.

From the requirement of FJM control problem to follow the desired value, based on SCT for engineering systems, we propose the first technological invariant corresponding to the control objective:

$$x_1 = x_{sp}. \tag{8}$$

In the first step, based on the purpose of controlling and reducing the order of the system model according to SCT, the first manifold selected has the form:

$$\psi_1 = x_4 - \varphi_1(x_1, x_2, x_3). \tag{9}$$

In the manifold (9) contains the function $\varphi_1(x_1, x_2, x_3)$, which determines the desired properties of the link velocity $x_4$ at the intersection with the invariant manifold $\psi_1 = 0$. The function $\varphi_1(x_1, x_2, x_3)$ is calculated in the next steps, to ensure that it satisfies the technological invariant (8). According to SCT, to ensure that the manifold $\psi_1 = 0$ and satisfies the finite-time condition, the macro variable $\psi_1$ is chosen as the solution of the functional equation of the following form:

$$\dot{\psi}_1 + c_1 \operatorname{sgn}(\psi_1)\left|\psi_1\right|^{2\beta-1} + k_1\psi_1 = 0\,, \tag{10}$$

In there $c_1>0$, $k_1>0$ and $0.5 < \beta < 1$. Substituting (9) into (10) we have:

$$\frac{\mathrm{d}}{\mathrm{d}t}(x_4 - \varphi_1) + c_1 \operatorname{sgn}(\psi_1)\left|\psi_1\right|^{2\beta-1} + k_1\psi_1 = 0\,. \tag{11}$$

Substituting $\dot{x}_4$ in the system of equations (7) when $d = 0$ into (11), we obtain the control signal $u$ as follows:

$$u = \begin{pmatrix} -k(x_1 - x_3) + J\sum_{i=1}^{3}\dfrac{\partial\varphi_1}{\partial x_i}\dfrac{\mathrm{d}x_i}{\mathrm{d}t} \\ -J\left(c\operatorname{sgn}(\psi_1)\left|\psi_1\right|^{2\beta-1} + k_1\psi_1\right) \end{pmatrix} / N\,. \tag{12}$$

With the synthesis of the control law $u$ as described, after some time, the manifold $\psi_1$ will change and asymptotically stabilize to 0 (i.e., $x_4$ becomes $\varphi_1$). At this point, the dynamics of the initial system will become the dynamics of the following system:

$$\begin{cases} \dot{x}_1 = x_2; \\ \dot{x}_2 = -\dfrac{k}{I}x_1 - \dfrac{mgl}{I}\sin(x_1) + \dfrac{k}{I}x_3; \\ \dot{x}_3 = \varphi_1. \end{cases} \tag{13}$$

In the following steps, the synthesis process is carried out sequentially to determine the internal control signals $\varphi_1$, $\varphi_2(x_1, x_2)$ and the technological invariant (8). The manifolds are chosen sequentially to ensure system stability and convergence to the following manifolds: $\psi_2 = x_3 - \varphi_2$, $\psi_3 = x_2 - K(x_1 - x_{sp})$. These manifolds satisfy the following functional equations:

$$T_2\dot{\psi}_2 + \psi_2 = 0\,; \tag{14}$$

$$T_3\dot{\psi}_3 + \psi_3 = 0\,, \tag{15}$$

where $T_2$, $T_3$ are the positive constants.

With the synthesis steps as described above, the system will move to the final manifold $\psi_3$. When the system reaches the final manifold, it means that:

$$\psi_3 = 0 \Rightarrow x_2 - K(x_1 - x_{sp}) = 0\,. \tag{16}$$

The condition for (15) to be stable about $x_{sp}$ is $K<0$.

From equations (15) and (16), we find the internal control signals $\varphi_1$ and $\varphi_2$:

$$\varphi_1 = \sum_{i=1}^{2}\frac{\partial\varphi_2}{\partial x_i}\frac{dx_i}{dt} - \frac{x_3 - \varphi_2}{T_2}\,; \tag{17}$$

$$\varphi_2 = \frac{mgl}{I}\sin(x_1) + x_1 + \frac{IK}{k}(x_2 - \dot{x}_{sp}) - \\ - \frac{I}{kT_3}\left(x_2 - K(x_1 - x_{sp})\right). \tag{18}$$

From (12), (17) and (18), we find the control law $u$ for the FJM. To analyze the stability of system (7) with control law (12) and prove the stability time of the control system, we choose the Lyapunov function of the form:

$$V = \frac{1}{2}\psi_1^2\,. \tag{19}$$

Derivative of function (19) gets:

$$\dot{V} = \psi_1\dot{\psi}_1 = -\psi_1\left(c_1\operatorname{sgn}(\psi_1)\left|\psi_1\right|^{2\beta-1} + k_1\psi_1\right) = \\ = -c_1\left(\psi_1^{\,2}\right)^{\beta} - k_1\psi_1^{\,2} = -\frac{c_1}{2^{\beta}}V^{\beta} - \frac{k_1}{2}V \tag{20}$$

According to the Lyapunov method, $\psi_1 \to 0$ as $t \to \infty$. Combined with SCT $\psi_2 \to 0$, $\psi_3 \to 0$ and $x_1 \to x_{sp}$. Therefore, the system is asymptotically stable. From (20) and according to Lemma 1, the settling time to the first manifold from the initial position is calculated using (3).

**2.6 Adaptive synergetic control design.** In practice, control systems can be subject to model uncertainties and input disturbances. As presented in the mathematical model of the FJM above, the component of the actuating motor is not fully modeled. For this reason, the finite-time controller must be designed to counteract these input disturbances. A common approach is to design an adaptive control law, incorporating estimated values of uncertainties into the control law. In this section, an adaptive control law is designed to estimate the input disturbance $d$. The proposed adaptive controller is as follows:

$$u = \begin{pmatrix} -k(x_1 - x_3) - \hat{d} + J\sum_{i=1}^{3} \dfrac{\partial \varphi_1}{\partial x_i} \dfrac{\mathrm{d}x_i}{\mathrm{d}t} \\ -J\left( c\,\mathrm{sgn}(\psi_1)|\psi_1|^{2\beta-1} + k_1\psi_1 \right) \end{pmatrix} / N, \quad (21)$$

where $\hat{d}$ is the estimated value of $d$.

Consider the Lyapunov function as in (19). The derivative of function (19) with the controller (21) applied to the system (7) when the system enters the first manifold is given by:

$$\dot{V} = \left( -c_1\,\mathrm{sgn}(\psi_1)|\psi_1|^{2\beta-1} - k_1\psi_1 \right)\psi_1, \quad (22)$$

where $\tilde{d} = d - \hat{d}$ is the error between the input disturbance and the observed disturbance. The Lyapunov function for designing adaptive controller has the following form:

$$V_{ad} = V + \frac{1}{2}\gamma\tilde{d}^2, \quad (23)$$

where $\gamma$ is the positive constant.

The derivative of function (23), we have:

$$\dot{V}_{ad} = -\left( \tilde{d} + c_1\,\mathrm{sgn}(\psi_1)|\psi_1|^{2\beta-1} + k_1\psi_1 \right)\psi_1 + \gamma\tilde{d}\dot{\tilde{d}} = \\ = -\frac{c_1}{2^\beta}V^\beta - \frac{k_1}{2}V + \tilde{d}\left( \gamma\dot{\tilde{d}} - \psi_1 \right). \quad (24)$$

The adaptive controller is determined based on $\dot{V}_{ad}$ being negative:

$$\dot{\hat{d}} = \gamma\psi_1. \quad (25)$$

The function (25) becomes:

$$\dot{V}_{ad} = -\frac{c_1}{2^\beta}V^\beta - \frac{k_1}{2}V \le 0. \quad (26)$$

According to the Lyapunov method and SCT, the controller (21) with the adaptive law (25) ensures that the system (7) is asymptotically stable. The block diagram of the control system with the finite-time adaptive controller for the FJM is shown in Fig. 2.

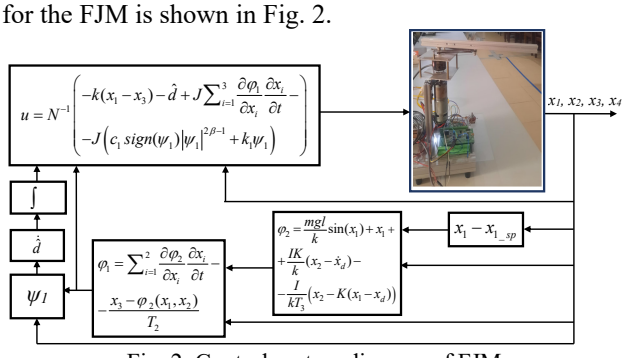


Fig. 2. Control system diagram of FJM

**3. Results and discussion.** In this section, to verify the effectiveness of the SCT law for flexible joints in the presence of input disturbances, different cases are conducted on numerical simulations and on the experimental model.

**3.1 Simulation results.** In the simulation, the FJM system is controlled according to the adaptive synergetic controller (21) implemented in MATLAB software. The model parameter values used in the simulation include: $m$ = 0.25 kg; $k$ = 20 N·m/rad; $J$ = 1 kg·m$^2$; $I$ = 0.2 kg·m$^2$; $g$ = 9.81 m/s$^2$; $l$ = 0.35 m; $N$ = 30 N·m/V. The parameters of the proposed control law (23) are as follows: $K$ = –90; $T_2$ = 0.12; $T_3$ = 0.12; $c_1$ = 100; $\beta$ = 0.9; $k_1$ = 100; $\gamma$ = 0.01. The input disturbance $d$ = 50 N·m. The simulation process of implementing the proposed finite-time adaptive synergetic control law is carried out with 2 cases: the first case, where the initial state of the system is at the origin $x_1 = 0$; $x_2 = 0$; $x_3 = 0$; $x_4 = 0$ moving to position $x_{1\text{–}sp} = \pi/2$; $x_{2\text{–}sp} = 0$; $x_{3\text{–}sp} = \pi/2$; $x_{4\text{–}sp} = 0$ in the first 5 s, and in the next 5 s, it moves to position $x_{1\text{–}sp} = -\pi/2$; $x_{2\text{–}sp} = 0$; $x_{3\text{–}sp} = -\pi/2$; $x_{4\text{–}sp} = 0$. The second case, where the initial position of the system is $x_1 = 0$; $x_2 = 0$; $x_3 = 0$; $x_4 = 0$ and then the link $q_1$ tracks the desired trajectory signal in the form $x_{1\text{–}sp} = \cos\omega t$ with the angular frequency $\omega$ = 1 rad/s. The maximum voltage applied to the motor is 12 V.

In the first case, the results indicate that the angle response of link $q_1(x_{1\text{–}pro})$ and $q_2(x_{3\text{–}pro})$ compared to the set value ($x_{1\text{–}sp}$) are shown in Fig. 3. From the graph, we see that the response of link $q_1$ stabilizes to the desired value with times of 0.495 s and 0.509 s, respectively (Table 1). The response of link $q_2$ shows oscillations during the transient process. This indicates that the actuator control signal adjusts quickly to ensure the system is stable within the given time according to Lemma 1. The difference in angle response between the two links and the set value is due to input disturbances and the flexible connection between the two links. The angular velocity response of link $q_2(x_{4\text{–}pro})$ is faster than link $q_1(x_{2\text{–}pro})$ to reduce the oscillation of link $q_1$. The control signal is clearly changing during the transient process to ensure the tracking performance of link $q_1$. The control signal does not return to zero because of the existence of the input disturbance $d$.

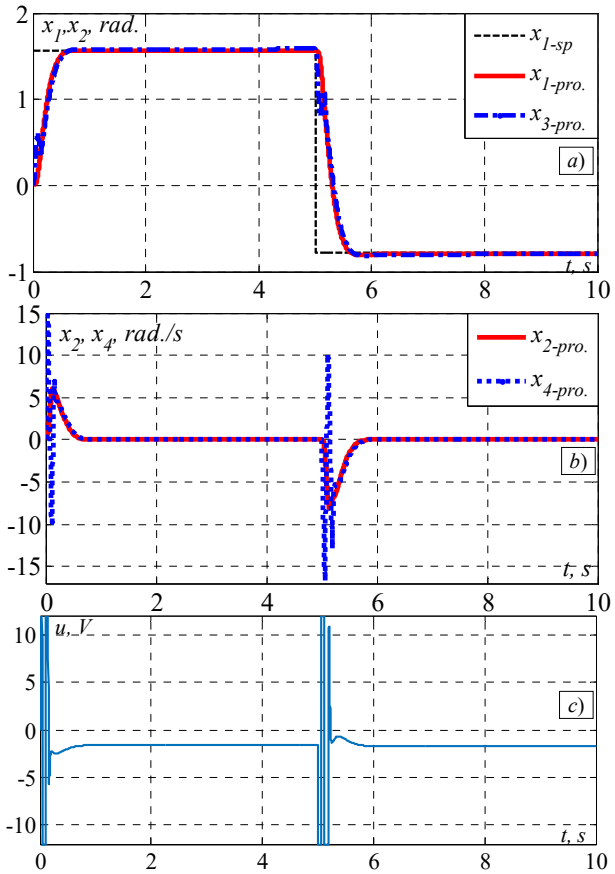


Fig. 3. Stability results in the first case with input disturbance: *a* – angle response; *b* – angular velocity response; *c* – control input

Table 1

Control system performance indicators

| $x_1$ | Time 0–5, s | | | Time 5–10, s | | |
|---|---|---|---|---|---|---|
| | $T_s$, s | $P.O.$, % | $e_{ss}$, rad | $T_s$, s | $P.O.$, % | $e_{ss}$, rad |
| | 0,495 | 0 | 0 | 0.509 | 0.8 | 0 |

*$T_s$ is the settling time; $P.O.$ is the percent overshoot; $e_{ss}$ is the steady-state error.

In the second case, the results indicate that the angle response of link $q_1$ tracking the setpoint signal and the angle of $q_2$ are shown in Fig. 4. From the graph, we can see that the response of link $q_1$ tracks the desired trajectory after 0.52 s. The response of link $q_2$ shows oscillations during the transient process, but eventually tracks the setpoint angle. During the transient process, the angular response oscillations indicate a change in the rotation direction of link $q_2$ to cancel out the oscillations in link $q_1$. The control signal with oscillations during the transient process and then following the periodic value of the setpoint signal once tracking is achieved.

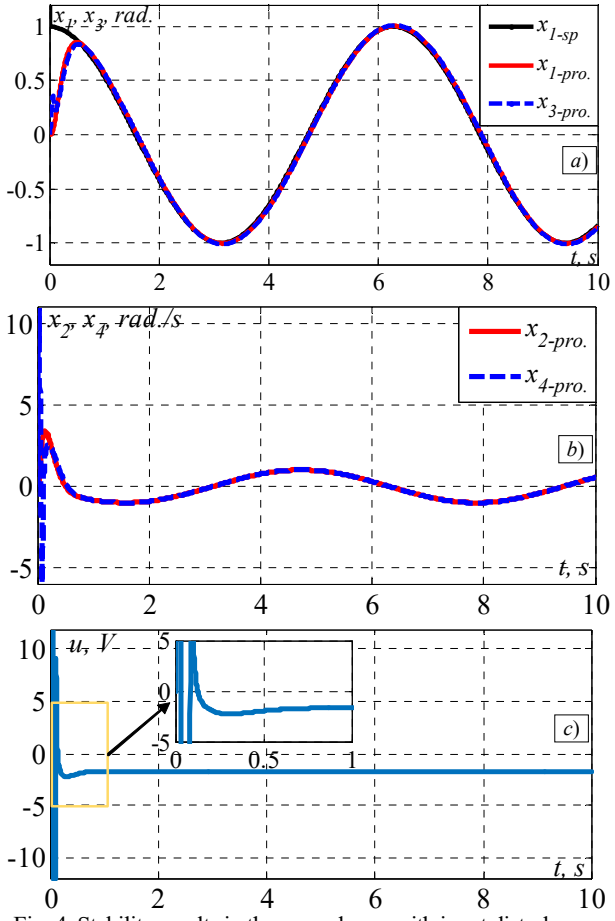


Fig. 4. Stability results in the second case with input disturbance: *a* – angle response; *b* – angular velocity response; *c* – control input

**3.2 Experimental verification.** To confirm the effectiveness of the proposed controller, experiments were conducted on the experimental model described in section 2 (Fig. 5). The control algorithms were implemented on STM32 cube IDE using C language with a sampling time of 2.5 ms. The experimental results of the proposed controller demonstrate the effectiveness of the proposed method without explicitly modeling the motor and input disturbances. In this case, model errors including of the motor and the controller, are inherent in the model. In the simulation section, these errors are considered as disturbance $d$. The dynamic parameters of the controller and the cases conducted are the same as in the simulation section.

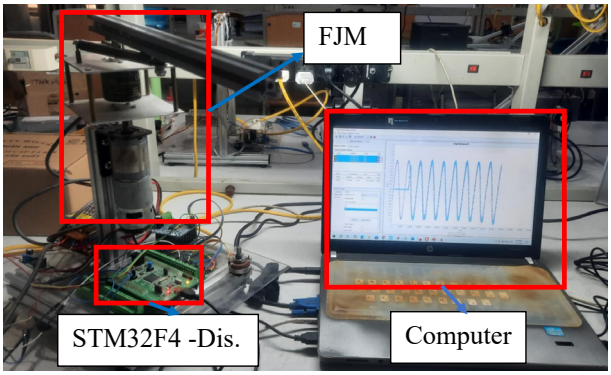


Fig. 5. Experimental platform FJM

The results presented in Fig. 6 show that the angle response of the FJM with the angle feedback of link $q_1$ stabilizes to the desired value. The angle response stabilizes to zero when the system is stable at the set value. The control signal supplied to the motor. Clearly, when stabilized at the balanced position, the voltage does not completely return to 0. This is due to various sources of disturbance such as friction, backlash in the gearbox, and joints, leading to the above errors. This also leads to the systems response not completely matching the simulation part.

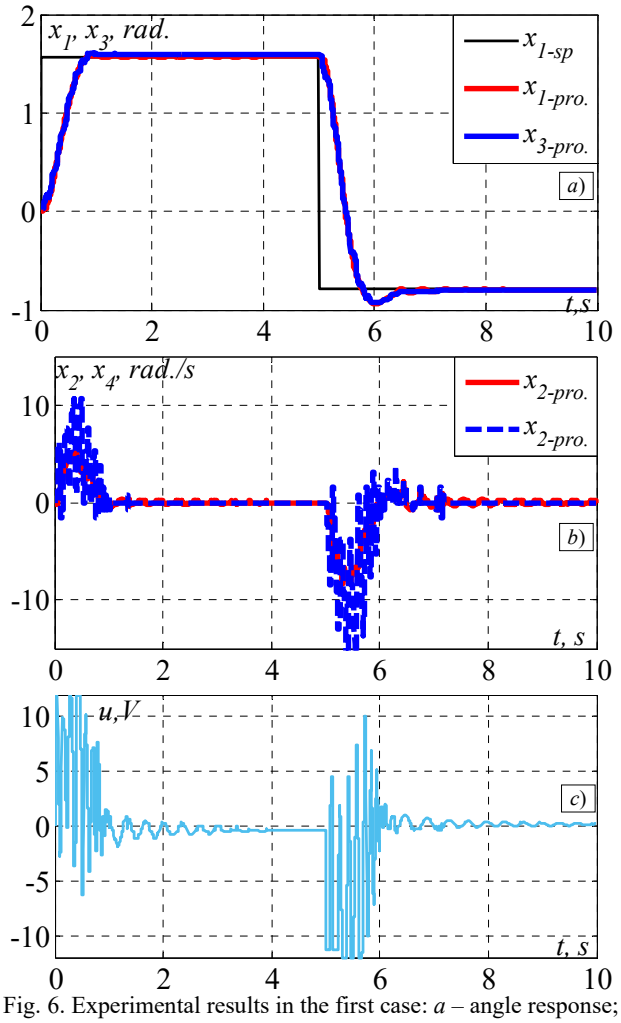


Fig. 6. Experimental results in the first case: *a* – angle response; *b* – angular velocity response; *c* – control input

The tracking performance on the experimental model is shown in Fig. 7. From the results, the angle of link $q_1$ tracks quite well. Besides, for the set-point signal in the form of an evaluation quantity, the response on the actual system is greatly affected by the motor with a gearbox. However, its results also show the possibility of realizing the controller appearing on real objects.

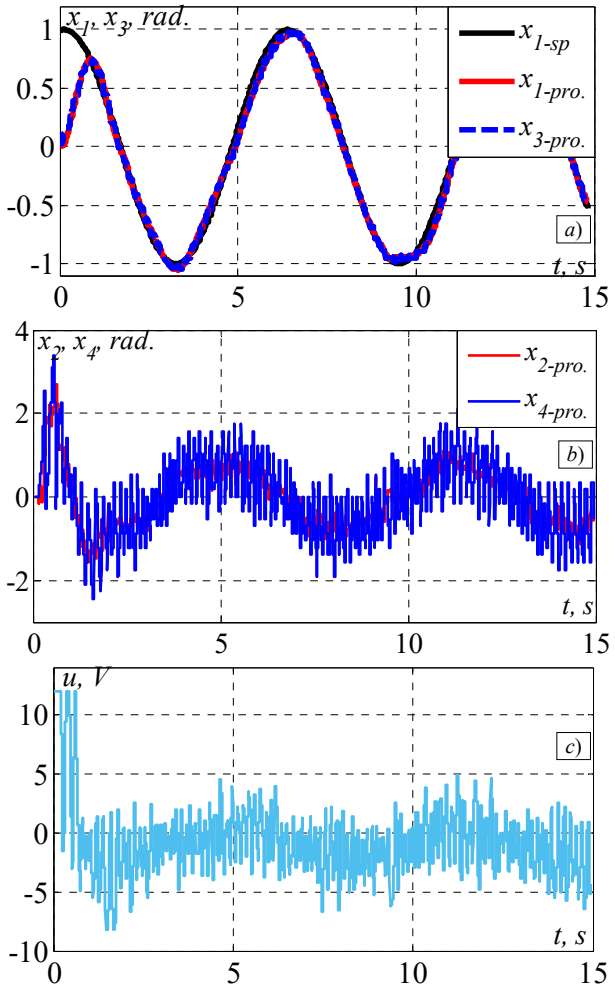


Fig. 7. Experimental results in the second case: *a* – angle response; *b* – angular velocity response; *c* – control input

**4. Conclusions.** The article presents the synthesis method of the finite-time adaptive synergetic control law for flexible joint systems. The synthesized control law ensures small system tracking errors and avoids oscillations. The finite-time characteristic is established based on the choice of the function equation. The developed adaptive law has well solved the problem of uncertainty in the mathematical model of the actuator and input disturbances. The stability of the system with the proposed control law is proven by the Lyapunov function. The simulation results of the proposed controller demonstrate its effectiveness. With two different tracking signal forms, the results show stability and tracking performance within a specified time. The results show that the system response has no oscillation and no overshoot. The proposed control law has been applied on the experimental model. Experimental results demonstrate the above tracking capability of the developed control method in the presence of input disturbances and without taking into account the mathematical model of the motor. Although the results on the actual system have limitations due to equipment quality and model uncertainty FJM, they also affirm the practical applicability of the control law. Finally, future researches will consider the effects of strong nonlinear disturbances from the actuator. It will also incorporate some modern theories such as fuzzy logic, neural networks, and nature-inspired optimization algorithms to fine-tune controller parameters and design the adaptive law.

**Conflict of interest**. The authors declare that they have no conflicts of interest.

REFERENCES


***1.*** Spong M.W., Hutchinson S., Vidyasagar M. Robot Modeling and Control. *Industrial Robot*, 2006, vol. 33, no. 5, 403 p.. doi: https://doi.org/10.1108/ir.2006.33.5.403.1.

***2.*** Wang Y., Guan Y., Li H. Observer-Based Finite-Time Sliding-Mode Control of Robotic Manipulator with Flexible Joint Using Partial States. *International Journal of Intelligent Systems*, 2023, vol. 2023, art. no. 8859892. doi: https://doi.org/10.1155/2023/8859892.

***3.*** Yan Z., Lai X., Meng Q., Zhang P., Wu M. Tracking control of single-link flexible-joint manipulator with unmodeled dynamics and dead zone. *International Journal of Robust and Nonlinear Control*, 2021, vol. 31, no. 4, pp. 1270-1287. doi: https://doi.org/10.1002/rnc.5335.

***4.*** Do T.-T., Vu V.-H., Liu Z. Linearization of dynamic equations for vibration and modal analysis of flexible joint manipulators. *Mechanism and Machine Theory*, 2022, vol. 167, art. no. 104516. doi: https://doi.org/10.1016/j.mechmachtheory.2021.104516.

***5.*** Cheng X., Liu H. Bounded decoupling control for flexible-joint robot manipulators with state estimation. *IET Control Theory & Applications*, 2020, vol. 14, no. 16, pp. 2348-2358. doi: https://doi.org/10.1049/iet-cta.2019.1007.

***6.*** Kivila A., Book W., Singhose W. Modeling spatial multi-link flexible manipulator arms based on system modes. *International Journal of Intelligent Robotics and Applications*, 2021, vol. 5, no. 3, pp. 300-312. doi: https://doi.org/10.1007/s41315-021-00201-3.

***7.*** Kumar P., Pratiher B. Nonlinear dynamic analysis of a multi-link manipulator with flexible links-joints mounted on a mobile platform. *Advances in Space Research*, 2023, vol. 71, no. 5, pp. 2095-2127. doi: https://doi.org/10.1016/j.asr.2022.10.031.

***8.*** Chiem N.X., Pham T.X., Thai P.D., Phan T.C. An Adaptive Sliding-mode Controller for Flexible-joint Manipulator. *2023 12th International Conference on Control, Automation and Information Sciences (ICCAIS)*, 2023, pp. 513-518. doi: https://doi.org/10.1109/ICCAIS59597.2023.10382364.

***9.*** Wang L., Shi Q., Liu J., Zhang D. Backstepping control of flexible joint manipulator based on hyperbolic tangent function with control input and rate constraints. *Asian Journal of Control*, 2020, vol. 22, no. 3, pp. 1268-1279. doi: https://doi.org/10.1002/asjc.2006.

***10.*** Gupta N., Pratiher B. Dynamic modeling and effective vibration reduction of dual-link flexible manipulators with two-stage cascade PID and active torque actuation. *Mechanism and Machine Theory*, 2025, vol. 205, art. no. 105867. doi: https://doi.org/10.1016/j.mechmachtheory.2024.105867.

***11.*** Hu Y., Dian S., Guo R., Li S., Zhao T. Observer-based dynamic surface control for flexible-joint manipulator system with input saturation and unknown disturbance using type-2 fuzzy neural network. *Neurocomputing*, 2021, vol. 436, pp. 162-173. doi: https://doi.org/10.1016/j.neucom.2020.12.121.

***12.*** Chang W., Li Y., Tong S. Adaptive Fuzzy Backstepping Tracking Control for Flexible Robotic Manipulator. *IEEE/CAA Journal of Automatica Sinica*, 2021, vol. 8, no. 12, pp. 1923-1930. doi: https://doi.org/10.1109/JAS.2017.7510886.

***13.*** Tang W., Chen G., Lu R. A modified fuzzy PI controller for a flexible-joint robot arm with uncertainties. *Fuzzy Sets and Systems*, 2001, vol. 118, no. 1, pp. 109-119. doi: https://doi.org/10.1016/S0165-0114(98)00360-1.

***14.*** Boussoffara M., Cheikh Ahmed I.B., Hajaiej Z. Sliding mode controller design: Stability analysis and tracking control for flexible joint manipulator. *Revue Roumaine Des Sciences Techniques Serie Electrotechnique et Energetique*, 2021, vol. 66, no. 3, pp. 161-167.

***15.*** Nam D.P., Loc P.T., Huong N. Van, Tan D.T. A Finite-Time Sliding Mode Controller Design for Flexible Joint Manipulator Systems Based on Disturbance Observer. *International Journal of Mechanical Engineering and Robotics Research*, 2019, vol. 8, no. 4, pp. 619-625. doi: https://doi.org/10.18178/ijmerr.8.4.619-625.

***16.*** Ali M., Mirinejad H. Robust tracking control of flexible manipulators using hybrid backstepping/nonlinear reduced-order active disturbance rejection control. *ISA Transactions*, 2024, vol. 149, pp. 229-236. doi: https://doi.org/10.1016/j.isatra.2024.04.026.

***17.*** Zhang Y., Zhang M., Fan C., Li F. A Finite-Time Trajectory-Tracking Method for State-Constrained Flexible Manipulators Based on Improved Back-Stepping Control. *Actuators*, 2022, vol. 11, no. 5, art. no. 139. doi: https://doi.org/10.3390/act11050139.

***18.*** Khan O., Mustafa G., Ashraf N., Hussain M., Khan A.Q., Shoaib M.A. Robust model predictive control of sampled-data Lipschitz nonlinear systems: Application to flexible joint robots. *European Journal of Control*, 2025, vol. 81, art. no. 101147. doi: https://doi.org/10.1016/j.ejcon.2024.101147.

***19.*** Ding S., Peng J., Zhang H., Wang Y. Neural network-based adaptive hybrid impedance control for electrically driven flexible-joint robotic manipulators with input saturation. *Neurocomputing*, 2021, vol. 458, pp. 99-111. doi: https://doi.org/10.1016/j.neucom.2021.05.095.

***20.*** Thang L.T., Son T.V., Khoa T.D., Chiem N.X. Synthesis of sliding mode control for flexible-joint manipulators based on serial invariant manifolds. *Bulletin of Electrical Engineering and Informatics*, 2023, vol. 12, no. 1, pp. 98-108. doi: https://doi.org/10.11591/eei.v12i1.4363.

***21.*** Benbouhenni H., Lemdani S. Combining synergetic control and super twisting algorithm to reduce the active power undulations of doubly fed induction generator for dual-rotor wind turbine system. *Electrical Engineering & Electromechanics*, 2021, no. 3, pp. 8-17. doi: https://doi.org/10.20998/2074-272X.2021.3.02.

***22.*** Cheng X., Zhang Y., Liu H., Wollherr D., Buss M. Adaptive neural backstepping control for flexible-joint robot manipulator with bounded torque inputs. *Neurocomputing*, 2021, vol. 458, pp. 70-86. doi: https://doi.org/10.1016/j.neucom.2021.06.013.

***23.*** Khatir A., Bouchama Z., Benaggoune S., Zerroug N. Indirect adaptive fuzzy finite time synergetic control for power systems. *Electrical Engineering & Electromechanics*, 2023, no. 1, pp. 57-62. doi: https://doi.org/10.20998/2074-272X.2023.1.08.

***24.*** Mahgoun M.S., Badoud A.E. New design and comparative study via two techniques for wind energy conversion system. *Electrical Engineering & Electromechanics*, 2021, no. 3, pp. 18-24. doi: https://doi.org/10.20998/2074-272X.2021.3.03.

***25.*** Truong H.V.A., Phan V.Du, Tran D.T., Ahn K.K. A novel observer-based neural-network finite-time output control for high-order uncertain nonlinear systems. *Applied Mathematics and Computation*, 2024, vol. 475, art. no. 128699. doi: https://doi.org/10.1016/j.amc.2024.128699.

*Received 25.10.2024*
*Accepted 26.01.2025*
*Published 02.05.2025*

*X.C. Nguyen* [1], *Doctor of Automatic Control,*
*D.T. Le*[2], *PhD of Automatic Control,*
[1] Department of Automation and Computing Techniques,
Le Quy Don Technical University, Hanoi, Vietnam,
e-mail: chiemnx@mta.edu.vn (Corresponding Author)
[2] Control, Automation in Production and Improvement of Technology Institute (CAPITI), Hanoi, Vietnam,
e-mail: ledanhtuan@gmail.com

*How to cite this article:*
Nguyen X.C., Le D.T. Adaptive finite-time synergetic control for flexible-joint robot manipulator with disturbance inputs. *Electrical Engineering & Electromechanics*, 2025, no. 3, pp. 45-52. doi: https://doi.org/10.20998/2074-272X.2025.3.07